The Identification of Quasars Behind Elliptical Galaxies and Clusters of Galaxies

Patricia M. Knezek ¹
Observatories of the Carnegie Institution of Washington, Las Campanas Observatory,
Casilla 601, La Serena, Chile
Electronic mail: pmk@pha.jhu.edu

and

Joel N. Bregman

Department of Astronomy, University of Michigan, Ann Arbor, MI 48109-1090

Electronic mail: jbregman@astro.lsa.umich.edu

ABSTRACT

The detection of resonance absorption lines against known objects such as individual galaxies and clusters of galaxies is a powerful approach for studying the gas content of these systems. We describe an efficient method of identifying background quasars suitable for absorption line studies. In this finding technique, we identify serendipitous X-ray sources, about 1/8 of which are suitably bright quasars at moderate redshift. We identify 16 new quasars and galaxies with active galactic nuclei (AGNs), and confirm 5 known quasars and AGNs, superimposed behind elliptical galaxies and clusters of galaxies. We also present 3 QSO/AGN candidates with uncertain redshift identifications.

Subject headings: galaxies; clusters; quasars; X-rays

1. Introduction

Our present understanding of the gaseous content of elliptical galaxies and of clusters of galaxies results largely from studies of the emission of photons from ionized plasmas and excited atoms. Studies of emission require that gas of particular temperature have

¹Now at the Department of Physics and Astronomy, The Johns Hopkins University, Baltimore, MD 21218-2695

an adequate emission measure, so it is insensitive to even large amounts of material for which the species are in their ground state. However, weakly excited gas can produce absorption lines against background continuum sources, so this gas can be detected, and with considerable sensitivity. In order to search for the absorbing gas, we have developed a strategy to identify background continuum sources, mostly quasars, behind elliptical galaxies and clusters of galaxies. The identification of this absorbing material not only improves our census of the interstellar content of these systems, it also tests several astrophysical models for its origin.

A variety of astrophysical events can occur in ellipticals and in clusters of galaxies that are unlikely to have a detectable emission signature but may lead to detectable absorption lines. For example, cooling and cooled gas is anticipated from the radiative losses (the X-rays) of the hot interstellar gas in these systems (e. g., from cooling flows, Fabian, Nulsen, and Canizares 1991; see also reviews by Fabbiano 1989 and Sarazin 1990). Two other sources for absorbing gas in elliptical galaxies are mass shed from evolving stars and accretion of gas onto the galaxy (Mathews and Baker 1971, Bregman 1978, White and Chevalier 1983). Important sources of absorbing gas in clusters of galaxies are from gas stripped out of galaxies (Gaetz, Salpeter, and Shaviv 1987) and infall of material into the cluster (Metzler 1995). The properties of the absorbing gas are often different for the various processes, so the detection of absorption lines can potentially identify the important processes in these systems.

Although many quasars are known, galaxies and clusters subtend a small solid angle on the sky, so there are relatively few coincidences with quasars. (Given the redshift range that we are searching for backgound objects, $z \sim 0.1-1$, we choose to use the terminology "quasar" in this paper, rather than active galactic nuclei (AGN) to designate emission line candidates.) Furthermore, most searches for quasars and active galactic nuclei avoided the region near bright galaxies. Therefore, there is a need to identify a reasonable number of new quasars near ellipticals and clusters of galaxies. These quasars should be bright enough to permit absorption line observations to be made with present telescopes, such as the Hubble Space Telescope (HST), in a reasonable amount of time (most of the quasars identified were scheduled for HST observations). Here we describe an effective technique for finding background quasars that makes efficient use of telescope time.

2. The Quasar Search Technique

It is valuable to understand the type of quasar needed for absorption line experiments in order to optimize a search technique. The most effective searches make use of resonance line absorption, and for the optical region, we are limited to Na I and Ca II. Not only are these uncommon species, but under many conditions, these will be poorly populated ionization states. Many of the most common elements, such as hydrogen, carbon, nitrogen, oxygen, iron, and magnesium, have resonance absorption lines in the ultraviolet region accessible by the HST. When one considers the abundance of the elements, the ionization state of the species, the spectral shape of quasars and the wavelength sensitivity of HST, the low ionization state gas is most readily detected by using the Mg II λ 2800Å doublet and the high ionization state gas from the C IV λ 1550Å doublet (Ly α is a special case). It is important that intrinsic features of the quasar not be confused with the features being searched for, so the Lyman alpha forest should not be shifted up to the wavelengths of these lines in the rest frame of the target galaxy or cluster. For low redshift clusters or galaxies, this places the restriction that $z_{qso} < 1.3$ to search for the Mg II lines and $z_{qso} < 0.27$ to search for C IV absorption.

This requirement on the redshift favors a quasar population whose mean redshift is < 1. Optically selected quasars have a mean redshift of ~1.5 (Hewett et al. 1995, Boyle et al. 1990) while radio selected quasars have a lower mean redshift of ~1.1 (Drinkwater et al. 1997), but X-ray selected quasars have a mean redshift of ~0.4 (Maccacaro et. al. 1991) to ~0.6 (Page et al. 1996), depending on the sensitivity of the survey. Even in deep X-ray surveys, the mean redshift of the X-ray selected quasars is only ~1.1 (Bower et al. 1996). Also, relatively few random optical sources are quasars, but approximately half of all X-ray point sources between energies of 0.5 and 2 keV are quasars (Boyle et al. 1994, 1997, Voges et al. 1996, Zhao et al. 1997). Furthermore, because there is a correlation of X-ray flux with optical and ultraviolet flux (Puchnarewicz et al. 1996, Walter and Fink 1993, Laor et al. 1994), X-ray selected quasars are preferentially bright in the ultraviolet region where the absorption line measurements will be made.

Our strategy has been to use X-ray images, largely from the ROSAT archives, of galaxies and clusters that are of interest. We search these fields for X-ray point sources and eliminate any sources that correspond to foreground Galactic stars, and in the clusters of galaxies, to a known cluster member. Subsequently, we try to identify the optical counterparts to these X-ray sources on the Digitized Sky Survey. There is a practical lower limit to the brightness of a useful quasar in that it must not require an inordinate amount of HST to detect absorption lines; this leads to V < 19.5 mag. X-ray targets whose optical counterpart is fainter than this limit are eliminated, and this removes about half of the potential targets. Typically there are $\sim 1-2$ good X-ray targets per ROSAT field searched.

The error circle associated with a particular X-ray detection depends on the instrument used, the characteristics of the particular field, and the strength of the X-ray point source.

Near the field center, the resolution of the two ROSAT instruments are 25" FWHM (PSPC) and 5" FWHM (HRI), and since it is possible to find the centroid to some fraction of the instrumental resolution, the centers can be located to about 10" for the PSPC and 2" for the HRI. However, the absolute positions given by the aspect solution for a particular field can be incorrect by as much as 15", although more typical values are 5-10". When there is an identified source in the field, such as a star, the position of the other sources can be corrected, leading to error circles of radius 10" for the PSPC and 5" for the HRI. When no source can be identified to correct the astrometry, we use an error circle of radius 20", which is conservative. With error circles of 20", there is usually no more than one object brighter than 19.5 mag within the circle. Once a target has been identified in this manner, the success rate of finding new quasars spectroscopically is about 50%, but their redshift may be too high or uncertain because only one emission line is seen, or their magnitude may have decreased below the limit. Approximately 1/4 sources that are observed with optical spectroscopy become acceptable targets for absorption line studies (1/8 of initial X-ray detections).

The angular distance on the sky between the galaxy or cluster being studied and the quasar depends upon the surface brightness of the emission from the cluster as well as on the exposure time of the X-ray field. For typical PSPC or HRI exposure times of 8-20 ksec, there are 2-3 quasars with z < 1.3 in 1000 square arcminutes (Page et al. 1996), most brighter than 19.5 mag. This is somewhat higher than optical searches, which typically find \sim 1 quasar in 1000 square arcminutes brighter than 19.5 magnitudes, assuming B-V=0.3(Boyle et al. 1990). However, for clusters of galaxies, the surface brightness of the cluster X-ray emission is fairly high and it is difficult to identify weak X-ray sources (potential background quasars) against this emission. Only the brighter X-ray quasars are visible through the inner regions of a cluster of galaxies, and for these identifications, the superior angular resolution of the HRI make these images more useful than the PSPC images, even though the HRI sensitivity is lower. Further from the cluster center (> 0.5 Mpc), where the cluster X-ray surface brightness is substantially lower, it is possible to identify fainter X-ray point sources for optical follow-up studies. In practice, for a typical bright X-ray cluster at a redshift of 0.05, the X-ray surface brightness is high in the inner 5-10', although we have been able to find quasars as close as 3' from the X-ray center of a cluster.

Similar considerations apply to elliptical galaxies, except that the region of high surface brightness is smaller (1-2') and many ellipticals are not particularly bright X-ray sources. In these cases, it has been possible to find background quasars within 2' of the center of the galaxy, although that was a exceptional case. For our sample, the median distance between an object, either the X-ray center of a cluster or an elliptical galaxy, and the closest detected quasar is 6-7'.

3. The Identification of New Quasars

3.1. The Sample

Our ongoing program searches for X-ray sources behind ellipticals, groups of galaxies, and clusters of galaxies. Our technique for the identification of background quasars has evolved and improved since we began this program and we do not claim that our search was complete to a particular X-ray flux or signal-to-noise limit. However, we have searched for quasar identifications for all 3σ X-ray sources within 8' of the cluster centers and all strong X-ray sources within 12' of the cluster center. Also, we investigated all 3σ X-ray point sources within the optical radius (D₂₅) of the centers of the elliptical galaxies.

3.2. Observations

Spectroscopic observations were made at Michigan-Dartmouth-MIT Observatory on the 2.4 m telescope. The first run was from 4 - 6 March 1994 and used the Mark III spectrograph with a 2048x2048 thick CCD. We used a 300 l/mm grism with a blaze angle of 6400Å and a 1".17 slit. The scale is 0.488 "/pix for this detector, giving a nominal resolution of ~8Å and a spectral range from 4260 - 11070Å. The second run was from 1 - 3 December 1994 and the third run was from 17 - 22 May 1995. Both runs used the Mark III spectrograph with a 1024x1024 thinned CCD. We used a 300 l/mm grism with a blaze angle of 5400Å and a 1".17 slit. The scale is 0.781 "/pix for this detector, giving a nominal resolution of ~8Å and a spectral range from 3620 - 9040Å (December 1994) and 3860 - 9352 Å (May 1995). Spectrophotometric standards were selected from Massey et. al. (1988) and Massey and Gronwell (1990). Images were bias subtracted and then flat-fielded using quartz lamp flats. An illumination correction was applied using dusk sky flats. Wavelength solutions were determined from Hg-Ne lamps, and no significant shift as a function of position on the sky was seen.

The X-ray sources identified as quasars are listed in Table 1. Column 1 lists the name, column 2 lists the foreground or background galaxy or cluster, columns 3 and 4 list the right ascension and declination in J2000, column 5 lists the quasar redshift, column 6 lists the spectroscopic visual magnitude, column 7 lists the date of the optical observation, column 8 lists the distance from the galaxy or cluster (X-ray center) in arcminutes, and column 9 lists the X-ray count rates for the detected quasars in 10⁻³ counts s⁻¹ (vignetting corrected) when available. The X-ray count rates were determined from the High Energy Astrophysics Science Archive Research Center (HEASARC) searches of the ROSAT Catalog PSPC RX MPE Sources (HEASARC-ROSATSRC) and ROSAT Catalog PSPC WGA

Sources (HEASARC_WGACAT), or were calculated from archived data by one of us (J. Bregman). In the cases where the source was detected in both catalogs (QSO0152-137, TON1480), the reported count rate is an average of the two given count rates. Sources without available X-ray counts were either taken from the Hewitt-Burbidge QSO catalog (1993, QSO0020+287 and QSO1124+271), discovered serendipitously in the spectrum of another source (QSO0109-153), or located more than 20 arcseconds from the X-ray source and therefore probably not associated with the X-ray source (QSO1201+580). For completeness, all quasars are listed, not just those in the proper magnitude or redshift range. It should be noted that the visual magnitudes listed are of varying accuracy, with those noted as definitely nonphotometric to be considered as upper limits. Furthermore, since the standards were taken through a narrow slit, the magnitudes are relative, not absolute. For a small number of sources which have also been imaged in V, the mean difference in V magnitude between the spectroscopic magnitude and photometric magnitude is 0.39 magnitudes. In the one case of an object whose spectrum was taken on a photometric night, the difference was 0.23 magnitudes. As a cautionary note, however, all the photometric data were taken at least a year after the spectroscopic data, and QSOs are known to vary by 0.1-0.4 magnitudes over weeks to years (Trevese et al. 1989, Kaspi 1997, Dietrich et al. 1997, Qian and Tao 1997), so the true errors are uncertain.

Finding charts are shown for the quasars in Figure 1. Each chart is 5' on a side, and north is up and east is to the left. The quasar is indicated by an arrow. The discovery spectra of the quasars are shown in Figure 2. Major emission lines are indicated. NS indicates a poorly subtracted night sky line.

The sources which were not identified as quasars are listed in Table 2. Column 1 lists the name. (In this case we have identified each object by "OBJxx±yy", where xx and yy are the full right ascension and declination. This was done because many of the observations are of objects only a few arcseconds apart.) Column 2 lists the corresponding foreground or background galaxy or cluster, columns 3 and 4 list the right ascension and declination in J2000, column 5 lists the date of the observation, and column 6 lists the source identification, if any. A search of the NASA Extragalactic Database² indicated that none of the non-AGN galaxies found in the course of this work were previously cataloged. Thus, we have also identified 8 new galaxies, most of which are probably previously unknown cluster members, based on their measured redshifts.

²The NASA/IPAC Extragalactic Database (NED) is operated by the Jet Propulsion Laboratory, California Institute of Technology, under contract with the National Aeronautics and Space Administration.

4. Conclusions

We have identified a successful process for locating quasar candidates behind individual galaxies and clusters of galaxies. Using X-ray images from archival data, we search for QSO candidates which are then identified via optical spectroscopy. We have presented 16 new quasars and galaxies with active galactic nuclei (AGNs), and confirmed 5 known quasars and AGNs. We also presented 3 QSO/AGN candidates with uncertain redshift identifications. We find that approximately 1/8 of X-ray identified sources prove to be QSOs with the correct redshift, spectral shape, and magnitude to be used in HST studies of the instellar and intergalactic media of galaxies and clusters of galaxies.

This research has made use of data obtained from the High Energy Astrophysics Science Archive Research Center (HEASARC), provided by NASA's Goddard Space Flight Center, and of the Digitized Sky Survey, as provided by the Space Telescope Science Institute. We are indebted to the staff at the Michigan-Dartmouth-MIT Observatory for their assistance and support in this matter. Also, we would like to thank Ken Banas for his assistance in identifying X-ray point sources in some of the fields. Finally, we wish to acknowledge support from NASA grants NAGW-2135 and NAGW-4448.

REFERENCES

- Argyle, R. W., and Eldridge, P. 1990, MNRAS, 243, 504.
- Bower, R. G., Hasinger, G., Castander, F. J., Aragón-Salamanca, A., Ellis, R. S., Gioia, I. M., Henry, J. P., Burg, R., Huchra, J. P., Böhringer, H., Briel, U. G., and McLean, B. 1996, MNRAS, 281, 59.
- Boyle, B. J., Fong, R., Shanks, T., and Peterson, B. A. 1990, MNRAS, 243, 1.
- Boyle, B. J., McMahon, R. G., Wilkes, B. J., and Elvis, M. E. 1994, MNRAS, 272, 462.
- Boyle, B. J., Wilkes, B. J., and Elvis, M. 1997, MNRAS, 285, 511.
- Bregman, J. N. 1978, ApJ, 224, 768.
- Dietrich, M., O'Brien, P. T., and Leighly, K. M. 1997, in "Emission Lines in Active Galaxies: New Methods and Techniques", eds. B. M. Peterson, F.-Z. Cheng, and A. S. Wilson (ASP: San Franciso), p. 163.

Drinkwater, M. J., Webster, R. L., Francis, P. J., Condon, J. J., Ellison, S. L., Jauncey, D. L., Lovell, J., Peterson, B. A., and Savage, A. 1997, MNRAS, 284, 85.

Fabian, A. C., Nulsen, P. E. J., and Canizares, C. R. 1991, A&A Rev., 2, 191.

Fabbiano, G. 1989, ARA&A, 27, 87.

Gaetz, T. J., Salpeter, E. E., and Shaviv, G. 1987, ApJ, 316, 530.

Giommi, P., Tagliaferri, G., Beuermann, K., Branduardi-Raymont, G., Brissenden, R., Graser, U., Mason, K. O., Mittaz, J. D. P., Murdin, P., Pooley, G., Thomas, H.-C., and Tuohy, I. 1991, ApJ, 378, 77.

Hewett, P. C., Foltz, C. B., and Chaffee, F. H. 1995, AJ, 109, 1498.

Hewitt, A., and Burbidge, G. 1993, ApJS, 87, 451.

Hill, J. M., and Oegerle, W. R. 1993, AJ, 106, 831.

Kaspi, S. 1997, in "Emission Lines in Active Galaxies: New Methods and Techniques", eds. B. M. Peterson, F.-Z. Cheng, and A. S. Wilson (ASP: San Franciso), p. 159.

Laor, A., Fiore, F., Elvis, M., Wilkes, B. J., and McDowell, J. C. 1994, ApJ, 435, 611.

Maccacaro, T., Della Ceca, R., Gioia, I. M., Morris, S. L., Stocke, J. T., and Wolter, A. 1991, ApJ, 374, 117.

Massey, P. and Gronwall, X. 1990, ApJ, 358, 344.

Massey, P., Strobel, K., Barnes, J., and Anderson, E. 1988, ApJ, 328, 315.

Mathews, W., and Baker, J. 1971, ApJ, 170, 241.

Metzler, C. 1995, Ph. D. Thesis, University of Michigan.

Oegerle, W. R., Hill, J. M., and Fitchett, M. J. 1995, AJ, 110, 32.

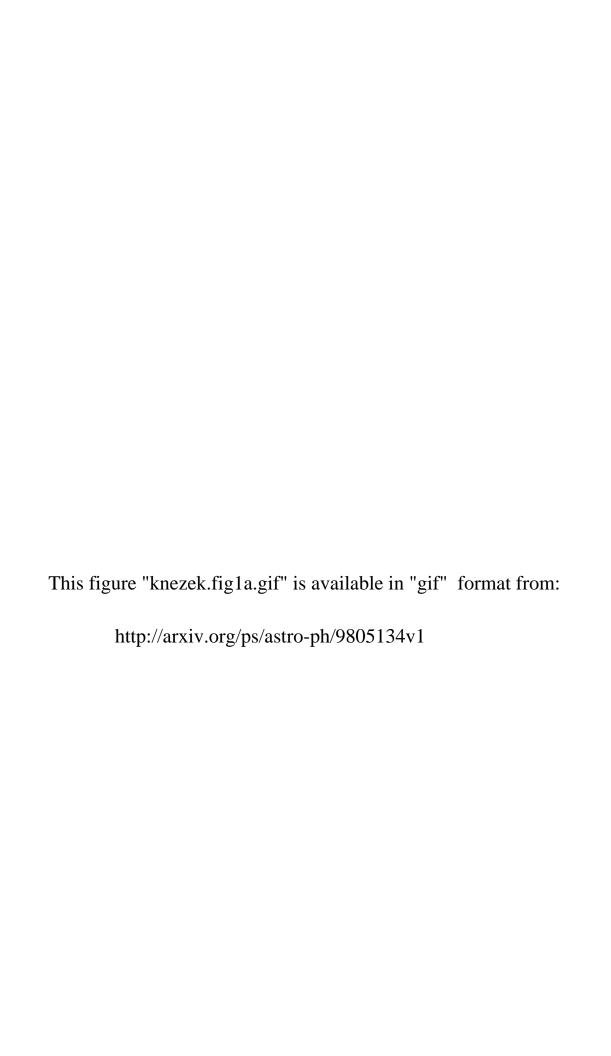
Page, M. J., Carrera, F. J., Hasinger, G., Mason, K. O., McMahon, R. G., Mittaz, J. P. D., Barcons, X., Carballo, R., González-Serrano, I., and Pérez-Fournon, I. 1996, MNRAS, 281. 579.

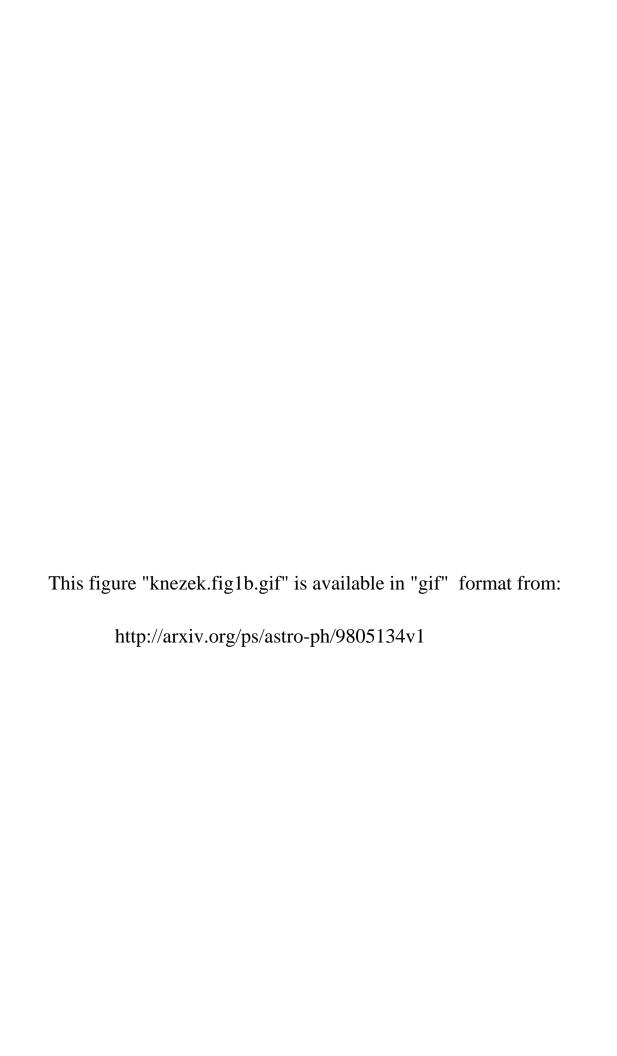
Puchnarewicz, E. M., Mason, K. O., Romero-Colmenero, E., Carrera, F. J., Hasinger, G., McMahon, R., Mittaz, J. P. D., Page, M. J., and Carballo, R. 1996, MNRAS, 281, 1243.

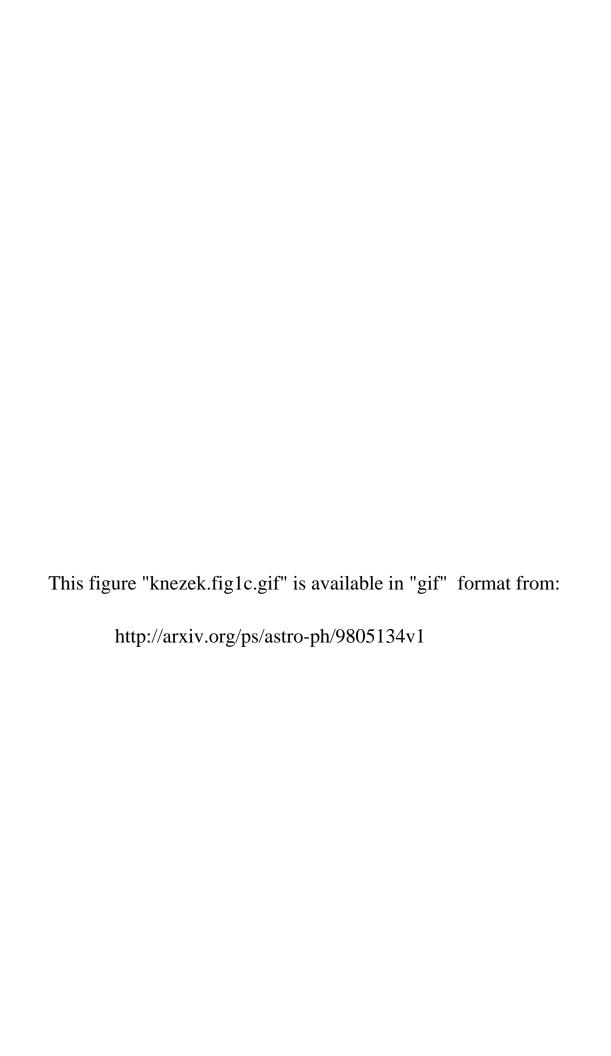
- Qian, B.-C. and Tao, J. 1997, in "Emission Lines in Active Galaxies: New Methods and Techniques", eds. B. M. Peterson, F.-Z. Cheng, and A. S. Wilson (ASP: San Franciso), p. 165.
- Sarazin, C. L. 1990, in "The Interstellar Medium of External Galaxies", eds. H. A. Thronson, Jr. and J. M. Shull (Dordrecht: Kluwer), p. 201.
- Trevese, D., Pittella, G., Kron, R. G., Koo, D. C., and Bershady, M. 1989, AJ, 98, 108.
- Voges, W., Boller, T., Dennerl, K., Englhauser, J., Gruber, R., Haberl, F., Paul, J., Pietsch, W., Trümper, J., and Zimmermann, H. U. 1996, in "Proceedings of 'Röntgenstrahlung from the Universe'", eds. H. U. Zimmermann, J. Trümper, and H. Yorke, MPE Report 263, p. 637.
- Walter, R., and Fink, H. H. 1993, A&A, 274, 105.
- White, R. E. III, and Chevalier, R. A. 1983, ApJ, 275, 69.
- Zhao, Y., Zhong, J., Wei, J., Hu, J., and Li, Q. 1997, in "Emission Lines in Active Galaxies: New Methods and Techniques", eds. B. M. Peterson, F.-Z. Cheng, and A. S. Wilson (ASP: San Franciso), p. 427.

This preprint was prepared with the AAS LATEX macros v4.0.

- Fig. 1a.— Finding charts for detected emission line objects. North is up and east is to the left. All charts are 5 arcminutes on a side. The object is indicated by an arrow.
- Fig. 1b.— Finding charts for detected emission line objects. North is up and east is to the left. All charts are 5 arcminutes on a side. The object is indicated by an arrow.
- Fig. 1c.— Finding charts for detected emission line objects. North is up and east is to the left. All charts are 5 arcminutes on a side. The object is indicated by an arrow.
- Fig. 1d.— Finding charts for detected emission line objects. North is up and east is to the left. All charts are 5 arcminutes on a side. The object is indicated by an arrow.
- Fig. 2a.— Discovery spectra for detected emission line objects. Major emission lines are indicated in each spectrum. NS indicates a poorly subtracted night sky line.
- Fig. 2b.— Discovery spectra for detected emission line objects. Major emission lines are indicated in each spectrum. NS indicates a poorly subtracted night sky line.
- Fig. 2c.— Discovery spectra for detected emission line objects. Major emission lines are indicated in each spectrum. NS indicates a poorly subtracted night sky line.







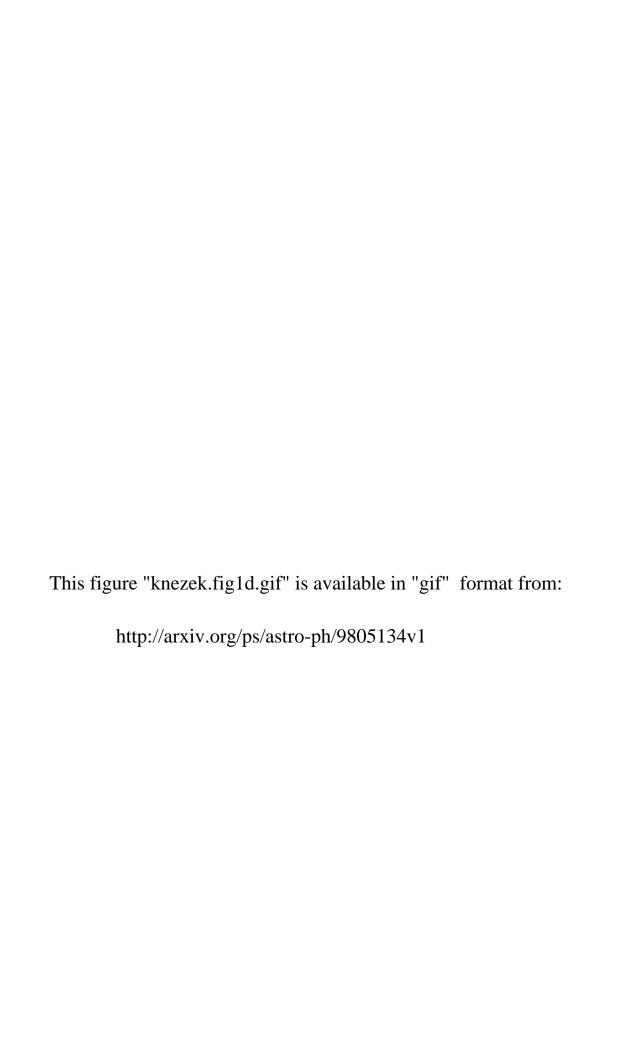


Table 1. X-ray Identified Quasars

Quasar	Foreground Source	α h m s	δ ° '/ '//	Z	m_V	Date of Observation	$D_{cen}(X)$	X-ray Count Rates 10^{-3} counts s ⁻¹
QSO0020+287	Abell 21	00:20:37.9	28:42:32	0.51	19.5	1 Dec 94	3.0	16.9
QSO0056-010	Abell 119	00:56:07.1	-01:03:41	0.17	19.1	$2 \mathrm{Dec} 94$	12.0	12.4
QSO0057 + 303	NGC 315	00:57:38.5	30:22:39	0.18	21.6	$1 \mathrm{Dec} 94$	4.0	2.6
${ m QSO}0107\text{-}156^{ m a}$	Abell 151	01:09:31.5	-15:21:51	0.86	$18.3^{\rm c}$	$3 \mathrm{Dec} 94$	10.0	
$\mathrm{QSO}0109\text{-}153^{\mathrm{e}}$	Abell 151	01:09:31.7	-15:20:41	0.049	$19.8^{\rm c}$	$3 \mathrm{Dec} 94$	10.0	
QSO0125+017	NGC 533	01:25:05.6	01:46:32	$0.75^{ { m b}}$	$19.6^{\rm c}$	$3 \mathrm{Dec} 94$	6.5	16.0
QSO0152-137	NGC 720	01:52:34.7	-13:47:35	0.17	19.2	$2 \mathrm{Dec} 94$	6.5	25.8
QSO0909-095	Abell 754	09:09:30.6	-09:32:22	0.63	$19.0^{ m d}$	$2 \mathrm{Dec} 94$	8.8	19.6
$QSO1124+271^{a}$	Abell 1267	11:27:36.3	26:54:51	0.379	17.0	17 May 95	5.7	
QSO1201 + 579	Abell 1446	12:01:04.5	57:58:48	1.84	$19.5^{ m d}$	21 May 95	8.5	3.5
QSO1201 + 581	Abell 1446	12:01:23.1	58:07:20	1.78	$20.0^{\rm c}$	19 May 95	7.4	6.4
QSO1201 + 580	Abell 1446	12:01:50.0	58:05:54	0.043	20.1	22 May 95	4.4	
TON 1480	NGC 4203	12:15:09.1	33:09:56	0.614	$16.4^{ m d}$	4 Mar 94	2.0	118.4
QSO1219+057	NGC 4261	12:19:49.0	05:45:33	0.113	$18.1^{ m d}$	5 Mar 94	6.0	10.4
QSO1225 + 182	NGC 4382	12:25:17.0	18:13:47	$1.19^{\rm b}$	$19.2^{ m d}$	5 Mar 94	2.9	8.8
QSO1225+183	NGC 4382	12:25:18.2	18:18:20	b	$18.9^{ m d}$	6 Mar 94	7.2	15.9
QSO1348 + 267	Abell 1795	13:48:15.6	26:44:45	0.93	19.9	17 May 95	12.0	22.1
$QSO1348 + 265^{f}$	Abell 1795	13:48:34.9	26:31:12	0.060	$15.6^{ m c}$	19 May 95	4.5	171.8
QSO1348 + 263g	Abell 1795	13:48:48.4	26:22:22	0.59	$18.8^{\rm c}$	18 May 95	13.0	55.4
QSO1354+402	HCG 68	13:54:20.4	40:12:39	1.39	19.6	22 May 95	11.2	4.3
QSO1454+186	Abell 1991	14:54:11.5	18:39:45	0.567	20.5	22 May 95	5.0	6.3
$QSO1511 + 057^{h}$	Abell 2029	15:11:33.6	05:45:48	0.086	$17.6^{\rm c}$	19 May 95	4.1	74.7
QSO1521 + 075	MKW = 3	15:21:15.6	07:30:31	1.44	$18.7^{\rm c}$	21 May 95	15.0	4.9
QSO1702+341	Abell 2244	17:02:26.1	34:11:19	0.108	16.7	22 May 95	8.0	49.9

^aKnown quasar from Hewitt-Burbidge QSO Catalog (1993) that was reobserved to obtain flux density and spectral slope.

 $^{^{\}rm b}{\rm QS\,O}0125+017\,$ is either at a redshift of 1.56 or 0.75. If it is at a redshift of 1.56, the emission lines at 5994Å and 8512Å remain unidentified. A more likely redshift is 0.75, but then H β at 8512Å is apparently very weak relative to H δ .

QSO1225+182 has only one line in the discovery spectrum, which is almost certainly Mg II, or other strong emission lines would be seen, hence the derived redshift.

QSO1225+183 has no obvious emission or absorption features, and may be a BL Lac object.

^cSpectra taken in non-photometric weather. Magnitudes are upper limits.

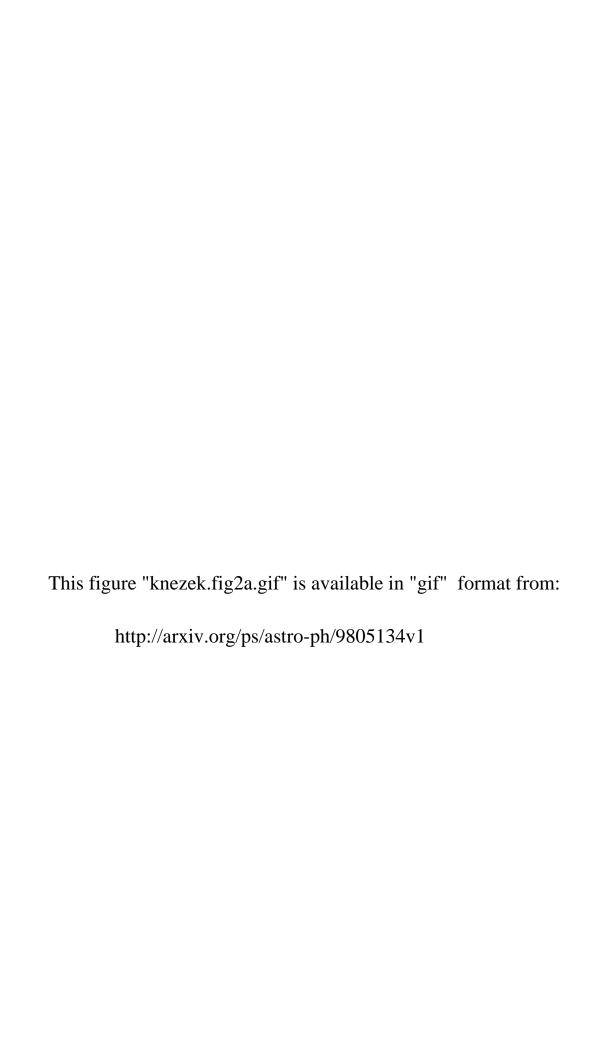
^dSpectra taken in possibly non-photometric weather. Magnitudes are uncertain by 0.4 magnitudes.

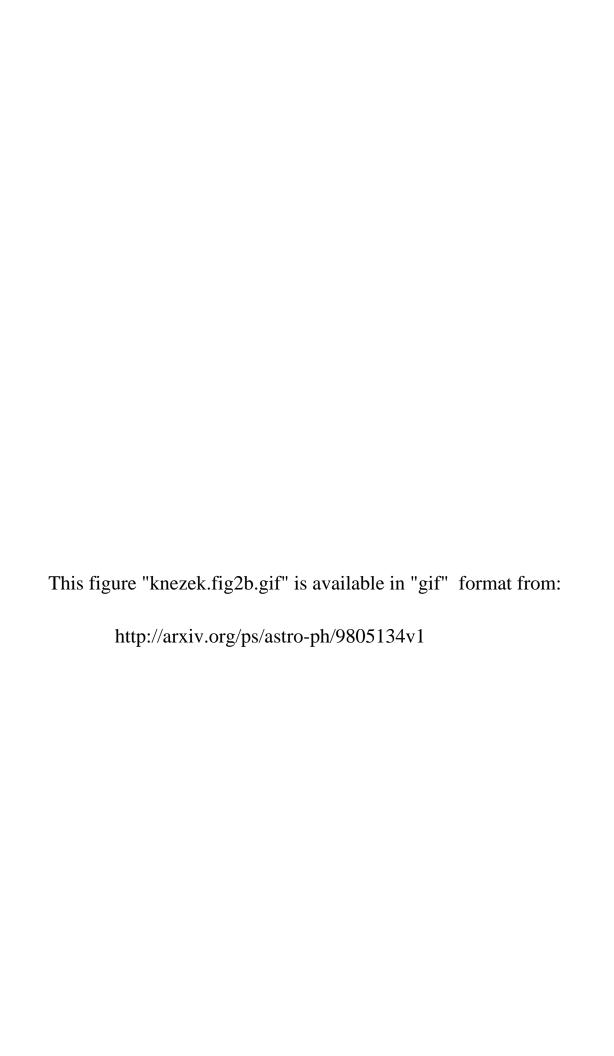
eAGN discovered when a known quasar was re-observed, offset 1.2' from the quasar.

f This AGN is LEDA 094626 (Argyle and Eldridge 1990), which has a measured redshift of z=0.05891 according to Hill and Oegerle (1993).

g This is the quasar EXO 1346.4+2637 (Giommi et al. 1991), for which they derive a redshift of z=0.59700.

^h This is the AGN Abell 2029 #272 (Oegerle et al. 1995), for which they derive a redshift of z=0.08492.





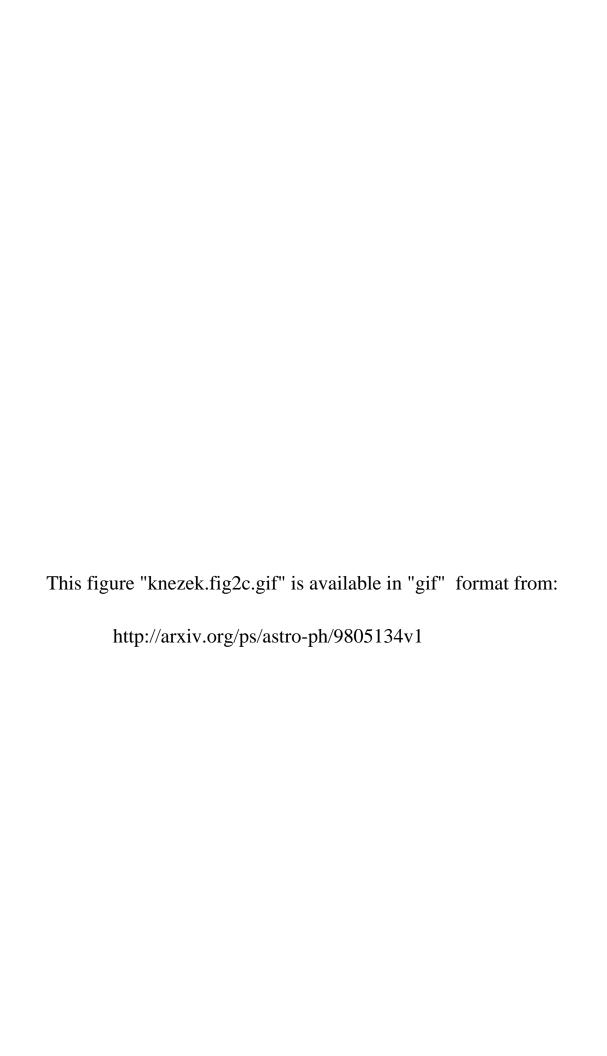


TABLE 2. Non-Emission Line Sources

Source	Foreground	α	δ	Date of	Source Identification
Sour se	Source	h m s	° <i>'</i>	Observation	
OBJ012536-012544	Abell 194	01:25:35.9	-01:25:44	3 Dec 94	galaxy, z~0.019
OBJ032614-212037	NGC 1332	03:26:14.5	-21:20:37	5 Mar 94	star
OBJ034030-183415	NGC 1407	03:40:29.6	-18:34:15	5 Mar 94	star
OBJ043325-131205	Abell 496	04:33:25.1	-13:12:05	2 Dec 94	star
OBJ044730-202031	Abell 514	04:47:30.2	-20:20:31	3 Dec 94	star
OBJ044731-201948	Abell 514	04:47:31.2	-20:19:48	2 Dec 94	galaxy, $z \sim 0.081$
$OBJ044837-202535^{a}$	Abell 514	04:48:37.1	-20:25:35	1 Dec 94	galaxy, z~0.071
OBJ090938-094137	Abell 754	09:09:37.7	-09:41:37	3 Dec 94	unknown, very weak
OBJ090939-094218	Abell 754	09:09:39.1	-09:42:18	2 Dec 94	galaxy, $z \sim 0.054$
OBJ090941-094130	Abell 754	09:09:41.0	-09:41:30	3 Dec 94	star
OBJ091033+595950	NGC 2768	09:10:32.7	+59:59:50	6 Mar 94	star
OBJ091040 + 595837	NGC 2768	09:10:40.3	+59.58:37	6 Mar 94	star
OBJ091049+600101	NGC 2768	09:10:48.7	+60:01:01	5 Mar 94	unknown, very weak
OBJ091050+600145	NGC 2768	09:10:49.7	+60:01:45	5 Mar 94	star
OBJ091056+600209	NGC 2768	09:10:56.2	+60:02:09	5 Mar 94	S/N very low, not reduced
OBJ091059+600041	NGC 2768	09:10:59.4	+60:00:41	4 Mar 94	star
OBJ091104+600102	NGC 2768	09:11:04.5	+60:01:02	5 Mar 94	star
OBJ115052-284355	NGC 3923	11:50:52.3	-28:43:55	6 Mar 94	uknown, very weak
OBJ115055-284322	NGC 3923	11:50:55.5	-28:43:22	4 Mar 94	star
OBJ115056-284333	NGC 3923	11:50:55.9	-28:43:33	4 Mar 94	star
OBJ115108-284713	NGC 3923	11:51:07.9	-28:47:13	5 Mar 94	star
OBJ115111-284639	NGC 3923	11:51:11.0	-28:46:39	5 Mar 94	star
OBJ115113-284734	NGC 3923	11:51:13.1	-28:47:34	6 Mar 94	star
OBJ120105 + 580324	Abell 1446	12:01:05.1	+58:03:24	21 May 95	star
OBJ120445 + 020118	MKW 4	12:04:45.2	+02:01:18	18 May 95	star
OBJ121506 + 331002	NGC 4203	12:15:05.6	+33:10:02	5 Mar 94	S/N very low, not reduced
OBJ121944 + 054533	NGC 4261	12:19:43.7	+05:45:33	5 Mar 94	unknown, very weak
OBJ121944 + 0544444	NGC 4261	12:19:44.5	+05:44:44	6 Mar 94	S/N very low, not reduced
OBJ122518 + 181912	NGC 4382	12:25:18.5	+18:19:12	6 Mar 94	star
OBJ122520+181401	NGC 4382	12:25:19.7	+18:14:01	6 Mar 94	S/N very low, not reduced
OBJ125255-091343	HCG 62	12.52.55.5	-09:13:43	20 May 95	uknown, very weak
OBJ125308-072403	HCG 62	12:53:08.0	-07:24:03	20 May 95	star
OBJ131136 + 391329	$Abell\ 1691$	13:11:36.3	+39:13:29	22 May 95	galaxy, $z \sim 0.074$
OBJ134830+601057	NGC~5322	13:48:29.8	+60:10:57	6 Mar 94	star
OBJ134841 + 601601	NGC~5322	13:48:40.9	+60:16:01	6 Mar 94	uknown, very weak
OBJ134859 + 601459	NGC 5322	13:48:59.2	+60:14:59	$4~{\rm Mar}~94$	uknown, very weak
OBJ152339 + 083337	Abell 2063	15:23:39.4	+08:33:37	20 May 95	galaxy, $z\sim0.029$
OBJ160135 + 161239	Abell 2147	16:01:35.5	+16:12:39	21 May 95	star
OBJ162714 + 394656	Abell 2199	16:27:14.0	+39:46:56	17 May 95	uknown, very weak
OBJ162724+405017	Abell 2197	16:27:23.8	+40:50:17	20 May 95	star
OBJ162825 + 405130	Abell 2197	16:28:25.0	+40.51:30	21 May 95	galaxy, $z\sim0.034$
OBJ162826 + 405143	Abell 2197	16:28:25.8	+40:51:43	21 May 95	star
OBJ171007+641241	Abell 2255	17:10:07.4	+64:12:41	21 May 95	star
OBJ171013+641241	Abell 2255	17:10:13.3	+64:12:41	21 May 95	star
OBJ171209+635859	Abell 2255	17:12:09.1	+63:58:59	19 May 95	galaxy, $z\sim0.079$
OBJ171326+641002	Abell 2255	17:13:25.6	+64:10:02	19 May 95	star

^aSource is extremely close to a bright star at α =04:48:35.5, δ =-20:25:43.